European Journal of Medicinal Chemistry 44 (2009) 1864–1869

Contents lists available at ScienceDirect

European Journal of Medicinal Chemistry

journal homepage: http://www.elsevier.com/locate/ejmech

Original article

The structure of Rimonabant in the solid state and in solution: An experimental and theoretical study

Ibon Alkorta [a], Mario Alvarado [a], José Elguero [a,*], Santiago García-Granda [b], Pilar Goya [a], María Luisa Jimeno [a], Laura Menéndez-Taboada [b]

[a] Instituto de Química Médica, CSIC, Juan de la Cierva, 3, E-28006 Madrid, Spain
[b] Dpto. de Química Física y Analítica, Facultad de Química, Universidad de Oviedo, E-33006 Oviedo, Spain

ARTICLE INFO

Article history:
Received 30 August 2008
Received in revised form
27 October 2008
Accepted 30 October 2008
Available online 5 November 2008

Keywords:
Rimonabant
X-ray structure
^{1}H NMR
^{13}C NMR
^{15}N NMR
DFT calculations
GIAO calculations

ABSTRACT

The X-ray molecular structure of Rimonabant methanol solvate has been determined together with the ^{1}H, ^{13}C and ^{15}N NMR spectra in acetone solution. B3YP/6-311++G(d,p) calculations have been performed out to determine two minimum energy conformations, on these geometries GIAO calculations were carried out to obtain the corresponding absolute shieldings that were compared with the experimental chemical shifts.

1. Introduction

Rimonabant (**1**) is the first selective CB1 receptor blocker used in patients of metabolic syndrome and related illness like diabetes and dyslipidaemia [1–4]. Our group has been active in this field preparing and evaluating a large series of compounds related to **1** [5–12]. A search in the crystallographic database (CSD) [13] shows that the structure of **1** was never reported and that very little is known about its NMR properties. Therefore, we decided (i) to determine its X-ray structure; (ii) to study its ^{1}H, ^{13}C and ^{15}N NMR spectra in solution, and (iii) to calculate its minimum geometry and the corresponding absolute shieldings. We hope doing this will provide other researches in the active field of cannabinoid antagonists with the molecular properties of the reference compound (Scheme 1).

A search in the CSD [13] was carried out to confirm that the structure of Rimonabant (**1**, SR 141716, CAS RN 168273-06-1) was not known. It is worth mentioning that there is a great interest on the polymorphism of **1** [14–18] but the X-ray molecular structure of none of the polymorphs has been solved, only power diffraction data were reported. Note also that no high-level computational study of compound **1** has been carried out; only molecular mechanics [19,20] and AM1 [21] calculations have been described.

2. Results and discussion

2.1. Crystallography

The structure of the methanol solvate of Rimonabant, shown in Fig. 1, displays no noticeable modifications in crystal packing from RT to 150 K. The solvate molecule helps to the packing connecting two Rimonabant molecules throughout the –N–H···O–H···O– synthon, forming infinite chains propagating along the *b* crystallographic axis. These strong interactions are shown in Tables 3 and 4 for the RT and 150 K, respectively. Two additional C–H···O– weak interactions shown in Table 4 were better located in the low temperature experiment.

2.2. NMR spectroscopy

The spectra were recorded in acetone-d_6 at 30 °C (^{1}H at 499.81 MHz), ^{13}C (125.68 MHz), ^{15}N (50.66 MHz) and the data reported in Table 1. The GIAO calculated absolute shieldings are also given in Table 1.

* Corresponding author. Tel.: +34 91 411 08 74; fax: +34 91 5644853.
E-mail address: iqmbe17@iqm.csic.es (J. Elguero).

0223-5234/$ – see front matter © 2008 Elsevier Masson SAS. All rights reserved.
doi:10.1016/j.ejmech.2008.10.037

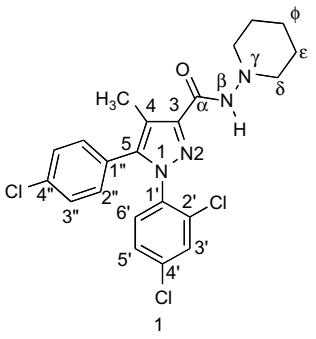

1

Scheme 1. Rimonabant.

These data are correlated through Eqs. (1a)–(5a) for **1a** and Eqs. (1b)–(5b) for **1b** which includes the three references (TMS ^{1}H, ^{13}C and $MeNO_2$ ^{15}N) calculated at the same level.

$$\delta^{15}N = -(136.8 \pm 3.2) - (0.907 \pm 0.028)\sigma^{15}N, \quad n = 5, r^2 = 0.997 \tag{1a}$$

$$\delta^{13}C = (172.6 \pm 1.5) - (0.944 \pm 0.016)\sigma^{13}C, \quad n = 19, r^2 = 0.995 \tag{2a}$$

$$\delta^{13}C = (175.4 \pm 0.8) - (0.964 \pm 0.009)\sigma^{13}C, \quad n = 16, r^2 = 0.999 \tag{3a}$$

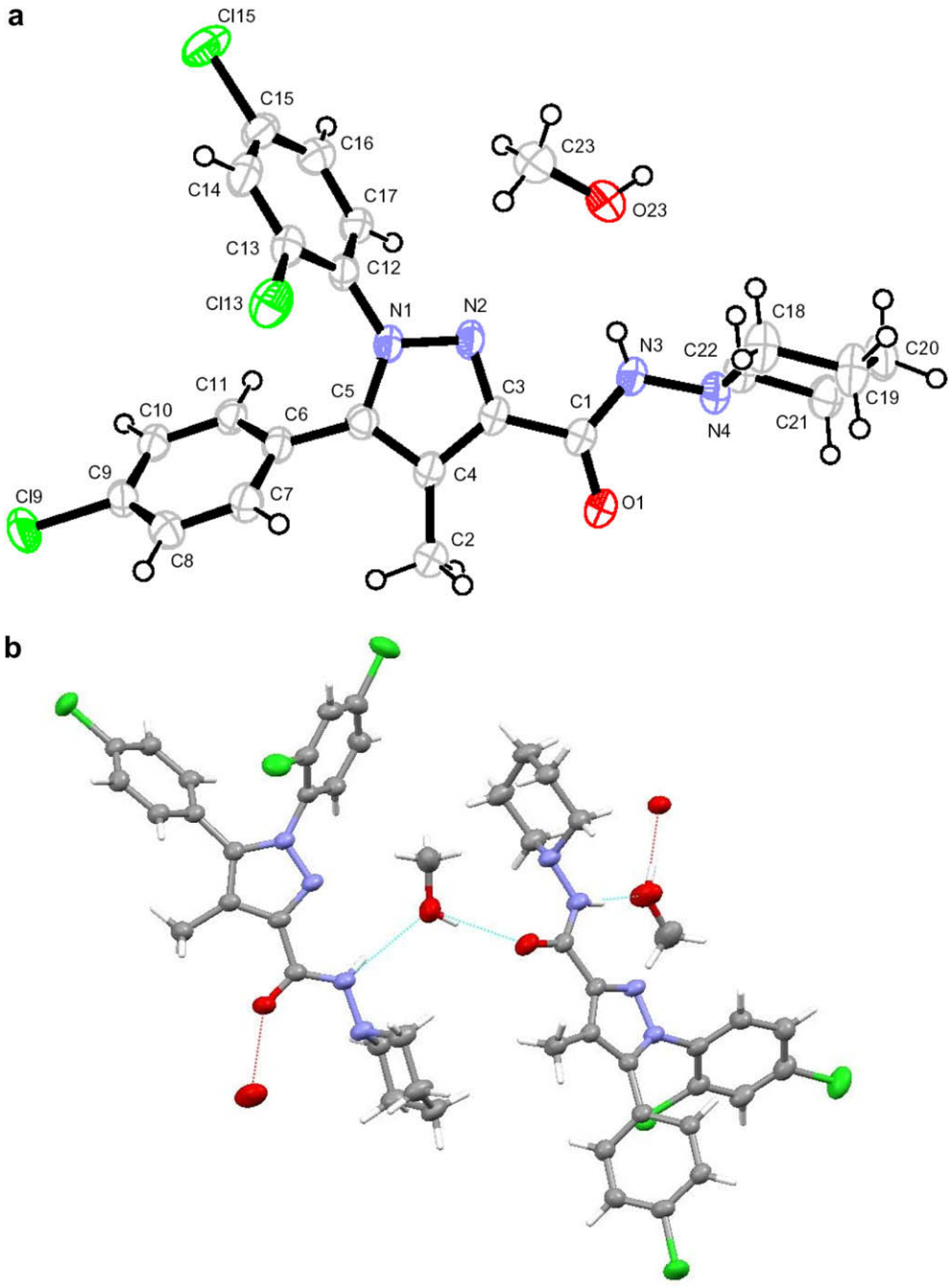

Fig. 1. Compound **1** at 150 K. Top: an isolated molecule (ORTEP). Bottom: the N3–H3···O23–H23···O1 hydrogen bond sequence (Mercury).

Table 1
Experimental (chemical shifts) and calculated (absolute shieldings) (ppm) and some coupling constants (Hz). Italicized values are the carbon atoms linked to chlorine atoms. Includes Ref. [22].

Experimental	Calculated **1a**	Calculated **1b**	^{1}H	^{15}N	^{13}C	^{1}H	^{15}N	^{13}C	^{1}H
Atom	^{15}N	^{13}C							
N1	−161.4	–	–	29.09	–	–	27.79	–	–
N2	−59.3	–	–	−78.41	–	–	−83.87	–	–
C3	–	144.87	–	–	31.42	–	–	31.94	–
C4	–	117.44	–	–	55.78	–	–	56.53	–
C–Me	–	8.82	2.30	–	171.62	29.55	–	171.54	29.55
C5	–	143.02	–	–	32.87	–	–	33.66	–
C1′	–	136.82	–	–	38.62	–	–	39.05	–
C2′	–	*132.92*	–	–	*34.92*	–	–	*33.35*	–
C3′	–	129.97	7.61	–	47.65	24.52	–	47.51	24.25
C4′	–	*135.78*	–	–	*32.55*	–	–	*32.19*	–
C5′	–	128.39	7.54	–	50.95	24.52	–	51.06	24.84
C6′	–	131.92	7.66	–	46.64	24.30	–	46.53	25.15
C1″	–	127.96	–	–	48.47	–	–	48.44	–
C2″	–	131.59	7.27	–	46.86	24.80	–	46.10	24.70
C3″	–	128.94	7.42	–	49.37	24.53	–	49.15	24.52
C4″	–	*134.59*	–	–	*33.43*	–	–	*32.19*	–
Cα	–	159.73	–	–	20.21	–	–	15.67	–
Nβ	−210.7[a]	–	8.21	91.26	–	24.79 (NH)	91.26	–	23.66 (NH)
Nγ	−284.4	–	–	154.20	–	–	154.20	–	–
CH_2 δ	–	56.16	2.90[b]	–	123.01	29.27		127.26	28.45
CH_2 ε	–	25.88	1.66[b]	–	153.48	30.18		152.41	30.32
CH_2 ϕ	–	23.50	1.41[b]	–	155.88	30.56		155.85	30.52
CH_3NO_2	0.00	–	–	−154.43	–	–	−154.43	–	–
TMS (^{13}C)	–	0.00	–	–	184.75	–	–	184.75	–
TMS (^{1}H)	–	–	0.00	–	–	31.97	–	–	31.97

[a] $J_{NH} = 95 \pm 3$ Hz.
[b] δ^{1}H (ppm) and J_{HH} [Hz] values for 10 proton system piperidine ring were obtained, assuming a rapid inversion of the ring in the NMR time scale, from spectral simulation using the gNMR program (Cherwell Scientific) [22] (Fig. 2). [δ CH_2, 4H, $J_{gem} = -12.1$, $^{3}J = 3.7$ and 7.0, ε CH_2, 4H, $J_{gem} = -13.5$, $^{3}J = 3.7$ and 8.0, ϕ CH_2, 2H, $J_{gem} = -12.5$].

$$\delta^{13}C = (175.4 \pm 0.8) - (0.964 \pm 0.008)\sigma^{13}C - (9.3 \pm 1.2)Cl, \quad n = 19, r^2 = 0.999 \tag{4a}$$

$$\delta^{1}H = (33.2 \pm 1.1) - (1.042 \pm 0.041)\sigma^{1}H, \quad n = 10, r^2 = 0.988 \tag{5a}$$

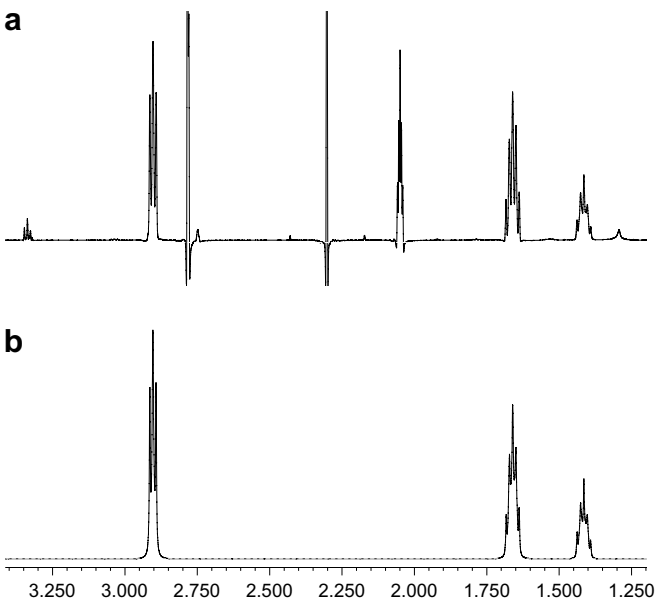

Fig. 2. 1D proton NMR experimental (a) and simulated spectrum (b) of the piperidine ring in compound **1** on the basis of the chemical shifts and coupling constants summarized in Table 1.

$$\delta^{15}N = -(135.3 \pm 1.9) - (0.904 \pm 0.017)\sigma^{15}N, \quad n = 5, r^2 = 0.999 \tag{1b}$$

$$\delta^{13}C = (173.0 \pm 1.4) - (0.951 \pm 0.016)\sigma^{13}C, \quad n = 19, r^2 = 0.995 \tag{2b}$$

$$\delta^{13}C = (175.7 \pm 0.8) - (0.969 \pm 0.009)\sigma^{13}C, \quad n = 16, r^2 = 0.999 \tag{3b}$$

$$\delta^{13}C = (175.7 \pm 0.8) - (0.969 \pm 0.008)\sigma^{13}C - (8.7 \pm 1.2)Cl, \quad n = 19, r^2 = 0.999 \tag{4b}$$

$$\delta^{1}H = (32.3 \pm 0.3) - (1.012 \pm 0.012)\sigma^{1}H, \quad n = 10, r^2 = 0.999 \tag{5b}$$

Eq. (3) corresponds to removing the three chlorine-bearing carbons that the calculations do not reproduce well [23]. Including a dummy for C–Cl atoms lead to Eq. (4) which shows that a correction of −9 ppm should be applied to these atoms. In the case of ^{1}H NMR we have excluded the NH signal too sensitive to solvent effects to obtain Eq. (5).

The correlations coefficients are equal or better using **1b** especially Eq. (5). Using only the five protons that are the most different for **1a** and **1b**, C3′H, C5′H, C6′H, CH_2δ and CH_2ε, Eq. (6) are obtained:

$$\delta^{1}H = (34.7 \pm 2.8) - (1.099 \pm 0.105)\sigma^{1}H, \quad n = 5, r^2 = 0.973 \tag{6a}$$

$$\delta^{1}H = (32.4 \pm 0.7) - (1.012 \pm 0.026)\sigma^{1}H, \quad n = 10, r^2 = 0.998 \tag{6b}$$

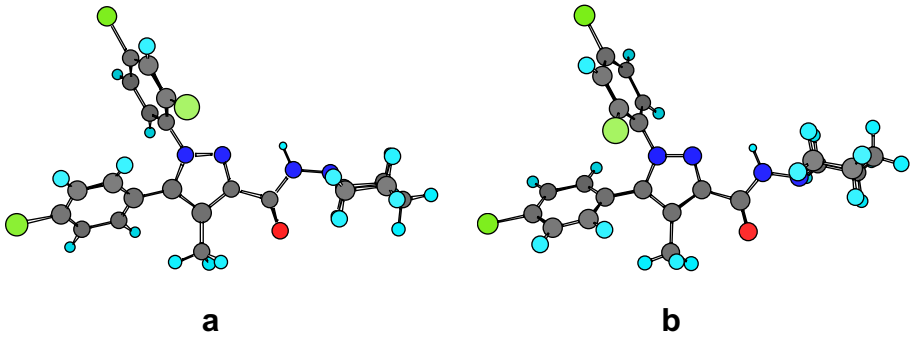

Fig. 3. Optimized structures of Rimonabant.

It is clear that although **1a** is more stable than **1b** in the gas phase (3.9 kJ mol^{-1}, see below), the NMR spectra in solution correspond to **1b**, the structure present in the crystal.

2.3. Computational studies

We have optimized the geometry of Rimonabant at the B3YP/6-311++G(d,p) level. We have used as starting geometry that of X-ray (Fig. 1). Compound **1** has five single bonds plus the conformation of the piperidine ring that should be optimized. The Cα–Nβ amide bond we have kept it fixed in the *Z* configuration, which is the standard one in the peptide bond [24]. The two phenyl rings are geared and their conformation limited by the presence of the methyl group in position 4 and the lone pair of N2.

(1) Concerning the C1′–N1 bond, there is only a minimum because rotating this bond only lead to a conformational mirror image.
(2) Rotation about the C1″–C5 bond produces the same conformation.
(3) Rotation about the C3–Cα bond from its planar *sE* configuration results in a large increase of the energy because in the planar *sZ* geometry there is a strong lone pair-lone repulsion (LP/LP) of the carbonyl oxygen atom and N2 [25]; besides the *sZ* configuration is stabilized by a Nβ–H···N2 hydrogen bond (the corresponding bond critical point is found in the AIM analysis [26]); this fix the C3–Cα/Cα–Nβ system of bonds.
(4) The most stable conformation of the 1-aminopiperidine ring is the chair with Nβ in equatorial position [27].
(5) We have rotated the Nβ–Nγ bond and found two minima **1a** and **1b** (Fig. 3) with a difference in energy of 3.9 kJ mol^{-1}, the less stable **1b** corresponding to the X-ray geometry (this difference in energy corresponds at 300 K to 83% **1a**/17% **1b**).

We have used both optimized geometries of Fig. 3 to calculate the absolute shieldings (GIAO) reported in Table 1.

The comparison of the calculated (**1b**) and experimental geometries (the RT and 150 K are almost identical) indicates that phase effects were negligible since all the corresponding torsion angles (the most sensitive parameter) were similar. For instance, the experimental dihedral angles f_1 (C2′–C1′–N1–C5) and f_5 (C2″–C1″–C5–N1) are 66.3/54.3° at RT and 65.3/54.2° at 150 K while the calculated ones are 68.9/50.8°, showing that the **1b** minimum energy conformation in the gas phase has a shape very similar to that found in the crystal. Also note that the presence of methanol in the crystal solvate has no appreciable effects on the structure.

Table 2
Crystal data and structure refinement for Rimonabant.

Temperature	293 K	150 K
Empirical formula	$C_{23}H_{25}Cl_3N_4O_2$	$C_{23}H_{25}Cl_3N_4O_2$
Formula weigh	495.82	495.82
Crystal system	Monoclinic	Monoclinic
Space group	*P* 21/*c*	*P* 21/*c*
a (Å)	7.529(5)	7.4410(1)
b (Å)	13.259(5)	13.0347(2)
c (Å)	24.937(5)	24.8402(3)
α (°)	90	90
β (°)	98.548(5)	97.457(1)
γ (°)	90	90
V (Å^3)	2461.7(19)	2388.90(6)
Z	4	4
μ (mm^{-1})	3.592	3.701
F(000)	1032.0	1032.0
Wavelength (Å)	1.54184	1.54184
Reflections collected	11528	11445
Unique reflections	4970	4822
R_{int}	0.0224	0.0224
$R_1[I > 2\sigma(I)]$	0.0517	0.0502
wR_2 (all data)	0.1617	0.1454

3. Conclusions

Although we have not carried out the exploration of the conformational hypersurface of Rimonabant, we have located two minima very close in energy (3.9 kJ mol^{-1}) one of them being that found in the solid state by crystallography. Moreover, the NMR spectra measured in acetone solution agree better with the X-ray structure **1b** than with that obtained rotating the N–N bond **1a**. We propose that the same structure **1a** present in the solid state exists, at least in greater extent, in solution. Both **1a** and **1b** fit the 3D model of the cannabinoid receptor we have described in 2005 [8]. We hope that these data will prove useful in the design of new drugs related with Rimonabant [3,28–30].

4. Experimental section

Rimonabant is a commercial product (Brain Research Chemicals International), two new synthetic methods have been described recently [31,32].

4.1. X-ray diffraction

A colorless crystal from Rimonabant was mounted on a Xcalibur Nova diffractometer and data were collected at 293(2) K and at 150(2) K using mirror-monochromated radiation CuK/α,

Table 3
Hydrogen-bonding geometry (Å, °) for Rimonabant at 293 K.

D–H···A	D–H (Å)	H···A (Å)	D···A (Å)	D–H···A (°)	Symmetry[a]
N3–H3···O23	0.85(3)	2.234(3)	3.047(4)	160(3)	
O23–H23···O1	0.82	2.02	2.790(1)	155.6	1

[a] Symmetry codes: (1) $-x,+y-1/2,-z+1/2+1$.

Table 4
Hydrogen-bonding geometry (Å, °) for Rimonabant at 150 K.

D–H···A	D–H (Å)	H···A (Å)	D···A (Å)	D–H···A (°)	Symmetry[a]
N3–H3···O23	0.79(4)	2.23(5)	2.985(4)	159(4)	
O23–H23···O1	0.80(5)	2.01(5)	2.764(4)	157(4)	1
C17–H17···O1	0.95	2.57	3.167(4)	121.1	2
C16–H16···O1	0.95	2.56	3.151(4)	120.6	2

[a] Symmetry codes: (1) $-x, -1/2+y, 3/2-z$; (2) $1-x, -1/2+y, 3/2-z$.

$\lambda = 1.54184$ Å. A total of 11528 ($-9 \le h \le 9$, $0 \le k \le 16$, $0 \le l \le 30$) resulting in 4970 independent reflections, [$R_{int} = 0.0224$], and 11445 ($-9 \le h \le 7$, $-16 \le k \le 15$, $-30 \le l \le 28$), 4822 independent reflections, [$R_{int} = 0.0224$], were collected and averaged at 293 K and 150 K, respectively. Data collection was made using the program CrysAllis CCD [33]. An empirical absorption correction [34] was applied to the intensity data. Crystal structures were solved by Direct Methods, using the program Sir92 [35]. Anisotropic least-squares refinement was carried out with SHELXL-97 [36]. Further details of the X-ray structural analysis are given in Table 2. Hydrogen bonds are listed in Tables 3 and 4 for the compound at both temperatures. Most H atoms were located by means of a final difference Fourier synthesis using the 150 K data. Relevant hydrogen atoms, H23 on the methanol molecule and H3 on the NH group, were isotropically refined. Geometrical calculations were made with PARST97 [37] and molecular graphics with ORTEP-3 [38] for windows. The structures at 150 and 293 K have been registered at the Cambridge Crystallographic Data Centre (CCDC 700181 and 700182, respectively).

4.2. Computational methods

The optimization of the geometries of the structures were first carried out at the B3LYP/6-31G* and then reoptimized at the B3LYP/6-311++G** computational level [39–44] within the Gaussian-03 package [45]. Frequency calculations at both levels were carried out to confirm that the obtained structures correspond to energy minima. GIAO absolute shieldings [46,47] were calculated on the B3LYP/6-311++G** optimized geometries.

4.3. NMR spectroscopy

^{1}H, ^{13}C and ^{15}N NMR spectra were recorded at 303 K, using acetone as the solvent, on a Varian SYSTEM 500 NMR spectrometer equipped with a 5 mm HCN cold probe. The chemical shifts are reported in ppm from tetramethylsilane but were measured against the solvent signals. All assignments have been performed on the basis of heteronuclear multiple quantum coherence experiments (gHMQC and gHMBC). Two-dimensional [^{1}H–^{13}C] NMR experiments (gHSQC and gHMBC) were obtained using a ^{1}H spectral window of 4808 Hz, a ^{13}C spectral windows of 30 000 Hz, 1 s of relaxation delay, 1024 data points, and 200 time increments, with a linear prediction to 512. The data were zero-filled to 4096 × 4096 real points. Typical numbers of transients per increment were 4 and 16, respectively. Two-dimensional [^{1}H–^{15}N] gHMBC experiment was carried out with the same conditions, using a ^{15}N spectral window of 15 200 Hz and 64 transients per increment.

Acknowledgements

This work was carried out with financial support from the Ministerio de Educación y Ciencia (Project No. CTQ2006-14487-C02-01/BQU) and Comunidad Autónoma de Madrid (Project MADRISOLAR, ref. S-0505/PPQ/0225). Mario Alvarado acknowledges a grant from RETICS RD06/001/0014 (Instituto de Salud Carlos III). SG-G gratefully acknowledges the financial support from MEC, projects MAT2006-01997 and Consolider Ingenio-2010, 'Factoría Española de Cristalización'.

References

[1] S.M. Wright, C. Dikkers, J.J. Aronne, Curr. Atheroscler. Rep. 10 (2008) 71–78.
[2] J. Elguero, P. Goya, N. Jagerovic, A.M.S. Silva, Targets in Heterocyclic Systems, vol. 6, 2002, pp. 52–96.
[3] N. Jagerovic, C. Fernández-Fernández, P. Goya, Curr. Topics Med. Chem. 8 (2008) 205–230.
[4] C.M. Chu, M.S. Hung, M.T. Hsieh, C.W. Kuo, T.D. Suja, C.W. Kuo, J.S. Song, H.H. Chiu, K.S. Shia, Org. Biomol. Chem. 6 (2008) 3399 and references therein.
[5] P. Goya, N. Jagerovic, Exp. Opin. Ther. Pat. 10 (2000) 1529–1538.
[6] P. Goya, N. Jagerovic, L. Hernández-Folgado, M.I. Martín, Mini Rev. Med. Chem. 3 (2003) 765–772.
[7] N. Jagerovic, L. Hernández-Folgado, I. Alkorta, P. Goya, M. Navarro, A. Serrano, F. Rodríguez de Fonseca, M.T. Dannert, A. Alsasua, M. Suardíaz, D. Pascual, M.I. Martín, J. Med. Chem. 47 (2004) 2939–2942.
[8] N.E. Campillo, C. Montero, P. Goya, J.A. Paéz, Eur. J. Med. Chem. 40 (2005) 75–83.
[9] N. Jagerovic, L. Hernández-Folgado, I. Alkorta, P. Goya, M.I. Martín, M.T. Dannert, A. Alsasua, J. Frigola, M.R. Cuberes, A. Dordal, J. Holenz, Eur. J. Med. Chem. 41 (2006) 114–120.
[10] F.J. Pavón, A. Bilbao, L. Hernández-Folgado, A. Cipitelli, N. Jagerovic, G. Abellán, M.I. Rodríguez-Franco, A. Serrano, M. Macías, R. Gómez, M. Navarro, P. Goya, F. Rodríguez de Fonseca, Neuropharmacology 51 (2006) 358–366.
[11] V.M.L. Silva, A.M.S. Silva, D.C.G.A. Pinto, N. Jagerovic, L.F. Callado, J.A.S. Cavaleiro, J. Elguero, Monatsch. Chem. 138 (2007) 797–811.
[12] F.J. Pavón, A. Serrano, V. Pérez-Valero, N. Jagerovic, L. Hernández-Folgado, F.J. Bermúdez-Silva, M. Macías, P. Goya, F.R. de Fonseca, J. Neuroendocrin. 20 (2008) 116–123.
[13] CSD database version 5.28 (November 2006). Jan-07 and May-07 updates F.H. Allen, Acta Crystallogr. Sect. B 58 (2002) 380–388; F.H. Allen, W.D.S. Motherwell, Acta Crystallogr. Sect. B 58 (2002) 407–422.
[14] A. Alcade, G. Anne-Archard, C. Gavory, O. Monnier, United States Patent 20050043356, Publication Date: 02/24/2005.
[15] J.S. Babu, G.J. Chavan, C.H. Khanduri, Eur. Pat. Appl. EP 1816125 A1 8 Aug 2007, Chem. Abstr. 147 (2007) 243166.
[16] V. Bolugoddu, V. Kotagiri, S. Kumar, S. Suthrapu, P. Kolkonda, R. Akula, A. Bhimireddy, PCT Int. Appl. WO 2007103711 A2 13 Sep 2007, Chem. Abstr. 147 (2007) 350666.
[17] H.M.H. Huang, C.G. Huang, U.S. Pat. Appl. Publ. US 2008004313 A1 3 Jan 2008, Chem. Abstr. 148 (2008) 106211.
[18] P. Reddy, R. Reddy, R. Reddy, M. Reddy, S. Chander Reddy, WO/2008/026219.
[19] M.E.Y. Francisco, H.H. Seltzman, A.F. Gilliam, R.A. Mitchell, S.L. Rider, R.G. Pertwee, L.A. Stevenson, B.F. Thomas, J. Med. Chem. 45 (2002) 2708–2719.
[20] B.F. Thomas, Y. Zhang, M. Brackeen, K.M. Page, S.W. Mascarella, H.H. Seltzman, AAPS J. 8 (2006) E665–E671.
[21] D.P. Hurst, D.L. Lynch, J. Barnett-Norris, S.M. Hyatt, H.H. Seltzman, M. Zhong, Z.-H. Song, J. Nie, D. Lewis, P.H. Reggio, Mol. Pharmacol. 62 (2002) 1274–1287.
[22] P.H.M. Budzelaar, g NMR Ver. 5.0 IvorySoft, Cherwell Scientific, Oxford, UK, 2004.
[23] (a) S. Fukawa, M. Hada, R. Fukuda, S. Tanaka, H. Nakatsuji, J. Comput. Chem. 22 (2001) 528–536; (b) R.M. Claramunt, C. López, M.A. García, M.D. Otero, M.R. Torres, E. Pinilla, S.H. Alarcón, I. Alkorta, J. Elguero, New J. Chem. 25 (2001) 1061–1068.
[24] L. Pauling, The Nature of the Chemical Bond, third. ed. Cornell University Press, 1960.
[25] R.W. Taft, F. Anvia, M. Taagepera, J. Catalán, J. Elguero, J. Am. Chem. Soc. 108 (1986) 3237.
[26] R.F.W. Bader, Atoms in Molecules. A Quantum Theory, Oxford University, New York, 1990.
[27] M. Oki, Applications of Dynamic NMR Spectroscopy to Organic Chemistry, VCH, Florida, 1985.
[28] M.E.Y. Francisco, J.P. Burgess, C. George, G.S. Bailey, A.F. Gilliam, H.H. Seltzman, B.F. Thomas, Magn. Reson. Chem. 41 (2003) 265–268.
[29] (a) J. Hodge, J.P. Bow, K.S. Plyler, V.K. Vemuri, A. Wisniecki, J.D. Salamone, A. Makriyannis, P.J. McLaughlin, Behav. Brain Res. 193 (2008) 285–305; (b) T.U.C. Järbe, B.J. LeMay, T. Olswewska, V.K. Vemuri, J.T. Wood, A. Makriyannis, Pharmacol. Biochem. Behav. 91 (2008) 84; (c) T.U.C. Järbe, C. Li, S.K. Subramanian, A. Makriyannis, Psychopharmacology 198 (2008) 467.
[30] M. Maccarrone, Br. J. Pharmacol. 153 (2008) 179–181.
[31] S.R. Donohue, C. Halldin, V.W. Pike, Tetrahedron Lett. 49 (2008) 2789–2791.
[32] T. Gustafson, F. Pontén, P.H. Seeberger, Chem. Comm. (2008) 1100–1102.
[33] Oxford Diffraction, 2008.
[34] S. Parkin, B. Moezzi, H. Hope, J. Appl. Crystallogr. 28 (1995) 53–56.
[35] A. Altomare, G. Cascarano, C. Giacovazzo, A. Guagliardi, M.C. Burla, G. Polidori, M. Camalli, J. Appl. Crystallogr. 27 (1994) 435–436.
[36] G.M. Sheldrick, SHELXL-97, Univ. of Gottingen, 1997.
[37] M. Nardelli, Comput. Chem. 7 (1983) 95–98.
[38] L.J. Farrugia, J. Appl. Crystallogr. 30 (1997) 565–566.
[39] A.D. Becke, Phys. Rev. A 38 (1988) 3098–3100.

[40] A.D. Becke, J. Chem. Phys. 98 (1993) 5648–5652.
[41] C. Lee, W. Yang, R.G. Parr, Phys. Rev. B 37 (1988) 785–789.
[42] P.A. Hariharan, J.A. Pople, Theor. Chim. Acta 28 (1973) 213–222.
[43] R. Ditchfield, W.J. Hehre, J.A. Pople, J. Chem. Phys. 54 (1971) 724–728.
[44] M.J. Frisch, J.A. Pople, R. Krishnam, J.S. Binkley, J. Chem. Phys. 80 (1984) 3265–3269.
[45] M.J. Frisch, G.W. Trucks, H.B. Schlegel, G.E. Scuseria, M.A. Robb, J.R. Cheeseman, J.A. Montgomery Jr., T. Vreven, K.N. Kudin, J.C. Burant, J.M. Millam, S.S. Iyengar, J. Tomasi, V. Barone, B. Mennucci, M. Cossi, G. Scalmani, N. Rega, G.A. Petersson, H. Nakatsuji, M. Hada, M. Ehara, K. Toyota, R. Fukuda, J. Hasegawa, M. Ishida, T. Nakajima, Y. Honda, O. Kitao, H. Nakai, M. Klene, X. Li, J.E. Knox, H.P. Hratchian, J.B. Cross, C. Adamo, J. Jaramillo, R. Gomperts, R.E. Stratmann, O. Yazyev, A.J. Austin, R. Cammi, C. Pomelli, J.W. Ochterski, P.Y. Ayala, K. Morokuma, G.A. Voth, P. Salvador, J.J. Dannenberg, V.G. Zakrzewski, S. Dapprich, A.D. Daniels, M.C. Strain, O. Farkas, D.K. Malick, A.D. Rabuck, K. Raghavachari, J.B. Foresman, J.V. Ortiz, Q. Cui, A.G. Baboul, S. Clifford, J. Cioslowski, B.B. Stefanov, G. Liu, A. Liashenko, P. Piskorz, I. Komaromi, R.L. Martin, D.J. Fox, T. Keith, M.A. Al-Laham, C.Y. Peng, A. Nanayakkara, M. Challacombe, P.M.W. Gill, B. Johnson, W. Chen, M.W. Wong, C. Gonzalez, J.A. Pople, Gaussian 03, Gaussian, Inc., Pittsburgh, PA, 2003.
[46] R. Ditchfield, Mol. Phys. 27 (1974) 789–807.
[47] F. London, J. Phys. Radium 8 (1937) 397–409.